

We are IntechOpen, the world's leading publisher of Open Access books Built by scientists, for scientists

4,800

Open access books available

122,000

International authors and editors

135M

Downloads

Our authors are among the

154

Countries delivered to

TOP 1%

most cited scientists

12.2%

Contributors from top 500 universities



WEB OF SCIENCE™

Selection of our books indexed in the Book Citation Index
in Web of Science™ Core Collection (BKCI)

Interested in publishing with us?
Contact book.department@intechopen.com

Numbers displayed above are based on latest data collected.

For more information visit www.intechopen.com



Quest for Lead-Free Perovskite-Based Solar Cells

Sajid Sajid, Jun Ji, Haoran Jiang, Xin Liu, Mingjun Duan, Dong Wei, Peng Cui, Hao Huang, Shangyi Dou, Lihua Chu, Yingfeng Li, Bing Jiang and Meicheng Li

Abstract

Today, the perovskite solar cells (PSCs) are showing excellent potentials in terms of simple processing, abundance of materials, and architectural integration, as well as very promising device's power conversion efficiencies (PCEs), rocketed from 3.8% in 2009 to 23.3% in 2018. However, the toxic lead (Pb) element containing the chemical composition of typically used organic-inorganic halide perovskites hinders the practical applications of PSCs. This chapter starts with a general discussion on the perovskite crystal structure along with the serious efforts focused on Pb replacement in these devices. Section 2 will elaborate the fundamental features of tin (Sn)-based perovskites together with their performance in the PSCs. Other alternative elements, such as copper (Cu), germanium (Ge), bismuth (Bi), and antimony (Sb), will be discussed in Section 3. The end will summarize the challenges and opportunities based on the chapter contents.

Keywords: toxicity, stability, lead-free perovskites, chemical composition

1. Introduction

PSCs with organometal (Pb) halide perovskites as photo-absorber showed rapid development in terms of PCEs from 3.8 to 23.3% [1–7]. The typically used Pb-based perovskites possess several appealing advantages such as broadband absorption range, long diffusion length, low exciton binding energy, and high-charge-carrier mobility [2, 3, 8–14]. However, intrinsic toxicity of Pb-based perovskites is a serious issue for both human and environment [15–19]. In this context, the replacement of Pb element in PSCs is extremely important for economical clean energy conversion devices which would benefit mankind in future endeavor.

Organic-inorganic trihalide perovskite is generally represented by ABX_3 ($A = CH_3NH_3^+$ (MA), $CH(NH_2)_2^+$ (FA), Cs^+ ; $B = Cu^{2+}$, Pb^{2+} , Sn^{2+} , Ge^{2+} , Bi^{3+} , Sb^{3+} ; $X = I^-$, Cl^- , Br^-). **Figure 1** illustrates the typical cubic perovskite structure with basic octahedron (BX_6) unit. It has been witnessed that structure distortions determine the physical/electrical properties of ABX_3 perovskite [20]. For example, Goldschmidt's tolerance prediction can be used for the dimensional evaluation of a perovskite as follows:

$$t = \frac{(r_A + r_X)}{\sqrt{2}(r_B + r_X)} \quad (1)$$

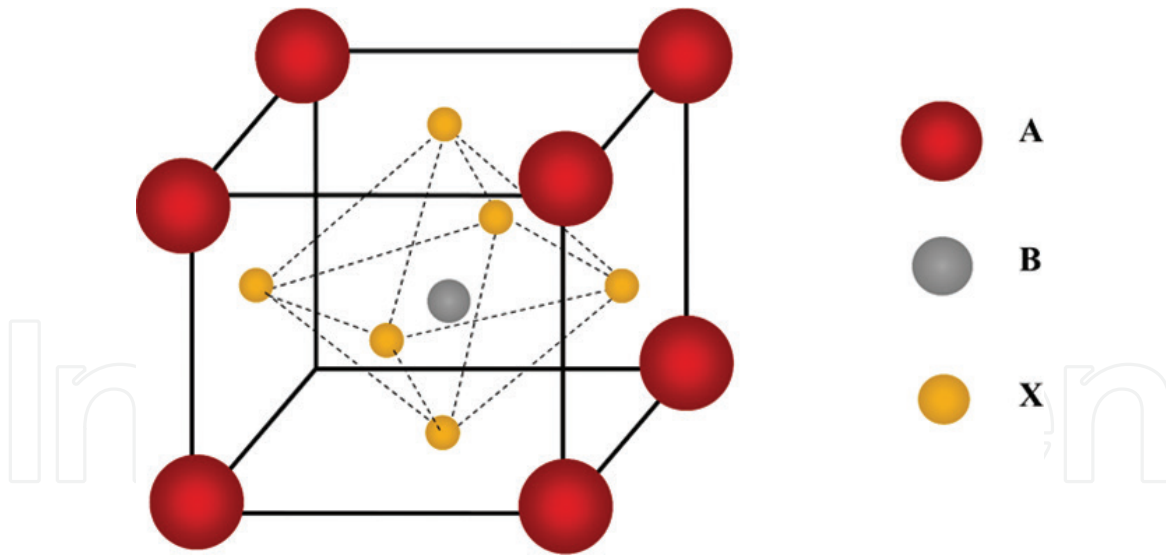


Figure 1.

Basic crystal structure of perovskite semiconductor, where A, B, and X represent $(\text{CH}_3\text{NH}_3^+, \text{CH}(\text{NH}_2)_2^+, \text{Cs}^+)$, $(\text{Cu}^{2+}, \text{Pb}^{2+}, \text{Sn}^{2+}, \text{Ge}^{2+}, \text{Bi}^{3+}, \text{Sb}^{3+})$, and $(\text{I}^-, \text{Cl}^-, \text{Br}^-)$, respectively.

where r_A , r_B , and r_X denote the ionic radii of A, B, and X, respectively. If the value of “ t ” results in the range between 0.813 and 1.107, then it is considered as a high-symmetry cubic three-dimensional (3D) perovskite, while two-dimensional (2D), one-dimensional (1D), and zero-dimensional (0D) perovskites are formed when “ t ” gives other values than the abovementioned range [21, 22]. The structural dimensionality approach is considered one of the essential factors because different dimensions of perovskite influence the kinetics of charge carriers. Nonetheless, this evaluation is not enough to be applied to all perovskite semiconductors. Therefore the probe for electronic dimensionality is equally important [23]. For example, perovskite materials with low electronic dimensionality but high structural dimensionality have less promises as light absorbers because of the barrier to isotropic current flow, large effective masses of holes/electrons, and deeper defect states.

The excellent performance of Pb-based perovskites is mainly due to high structural symmetry and strong antibonding coupling between Pb and I [24]. In a similar way, Cu^{2+} , Ge^{2+} , Bi^{3+} , Sb^{3+} , and Sn^{2+} with ns^2 lone pairs could be used with halides to obtain octahedral structure; therefore, they are investigated as alternatives to the toxic Pb element [15, 25, 26]. Herein, we will introduce the Pb-free perovskites from previously reported theoretical calculations and experimental studies.

2. Sn-based perovskites

Tin (Sn) element has been widely used as an alternative to Pb, since both occur in group IVA of the periodic table with similar ionic radii (Pb: 1.49 Å and Sn: 1.35 Å). Therefore, Pb substitution by Sn would cause no obvious lattice distortion in perovskites [27]. The intrinsic instability that results in the decomposition of unstable products such as SnI_2 and HI (acidifier) and toxicologically inactive oxygenated Sn precipitates are still remained the toxicity issues in the Sn-based perovskites [16]. However, benefiting from the stability of PSCs based on Sn perovskites and easy cleaning of Sn from the human body compared to Pb, Sn-based perovskites could be a better choice than perovskite with Pb cation. Density functional theory (DFT) and GW approximation are typically used for the structural and electrical properties of Sn-based perovskites [28, 29]. For instance, the theoretical–experimental calculations about the bandgap of MASnI_3 showed

a range of 1–1.3 eV, charge mobility of $1.6 \text{ cm}^2 \text{ V}^{-1} \text{ s}^{-1}$, and diffusion length up to 30 nm (**Figure 2A**) [29, 30, 32, 33]. Additionally, SnF_2 -doped MASnI_3 showed tenfold larger carrier lifetime with diffusion length of 500 nm (**Figure 2B**) [31]. Replacing MASnI_3 by FASnI_3 results in a desirable bandgap of 1.41 eV and minimized oxidation of Sn^{2+} to Sn^{4+} [34, 35]. It is also reported that replacement of “A” cation by Cs^+ in ASnX_3 yields higher charge mobility, lower exciton binding energy, and large optical absorption coefficient compared to conventional MAPbI_3 [36, 37]. However, plasticity of the tin-halide-tin angle and Cs^+ cation migration [38] showed CsSnX_3 a phase transitional perovskite with respect to temperature [39].

Since Sn-based perovskites possess low crystallization barrier and high solubility in solvents, their thin films can be fabricated at low temperature in the PSCs. For example, a high crystalline MASnI_3 -perovskite thin film has been prepared from a transitional $\text{SnI}_2 \cdot 3\text{DMSO}$ intermediate phase (**Figure 3A**) [40]. This high-quality perovskite film formation in a hole-selective layer-free PSCs resulted in a photocurrent of 21 mA cm^{-2} . In order to obtain low doping level in MASnI_3 -perovskite thin film, a low-temperature vapor-assisted solution process was employed (**Figure 3B**), where the excess of Sn^{2+} compounds due to $\text{Sn}(\text{OH})_2$ and SnO resulted in low hole-doping level [41, 44]. Furthermore, anti-solvent dripping process was used to control fast crystallization and fabricate pinhole-free thin films of Sn-based perovskites. The diethyl ether dripping on FASnI_3 and chlorobenzene on $(\text{FA})_{0.75}(\text{MA})_{0.25}\text{SnI}_3$ enabled the as-prepared PSCs to obtain efficiency of 6.2 and 8.1%, respectively (**Figure 3C and D**) [42, 43].

It is reported that the oxidation of Sn-based perovskites (self-doping from Sn^{2+} to Sn^{4+}) leads to carrier recombination and poor device performance. In this context, specific amount of SnF_2 can be used as an inhibitor for Sn^{4+} . The large quantity of SnF_2 may generate phase separation such as plate-like aggregates on the perovskite film surface. Here, the strong binding affinity in SnF_2 -pyrazine complex was helpful to

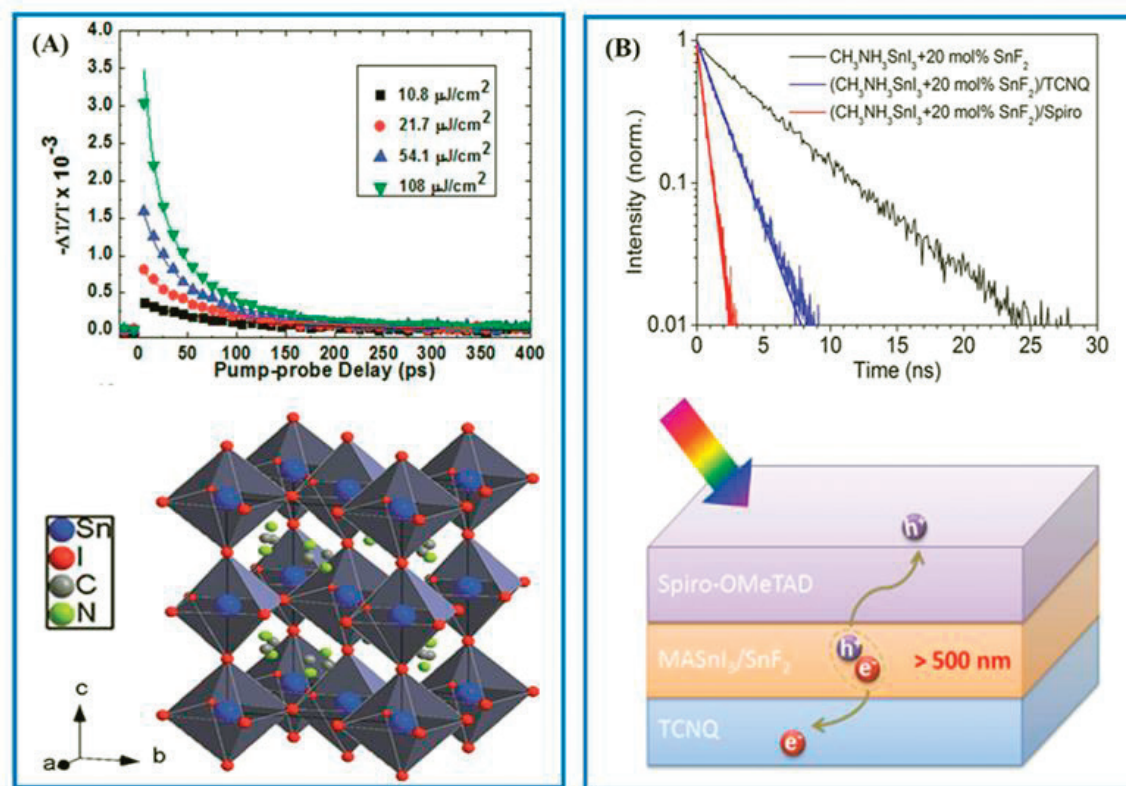
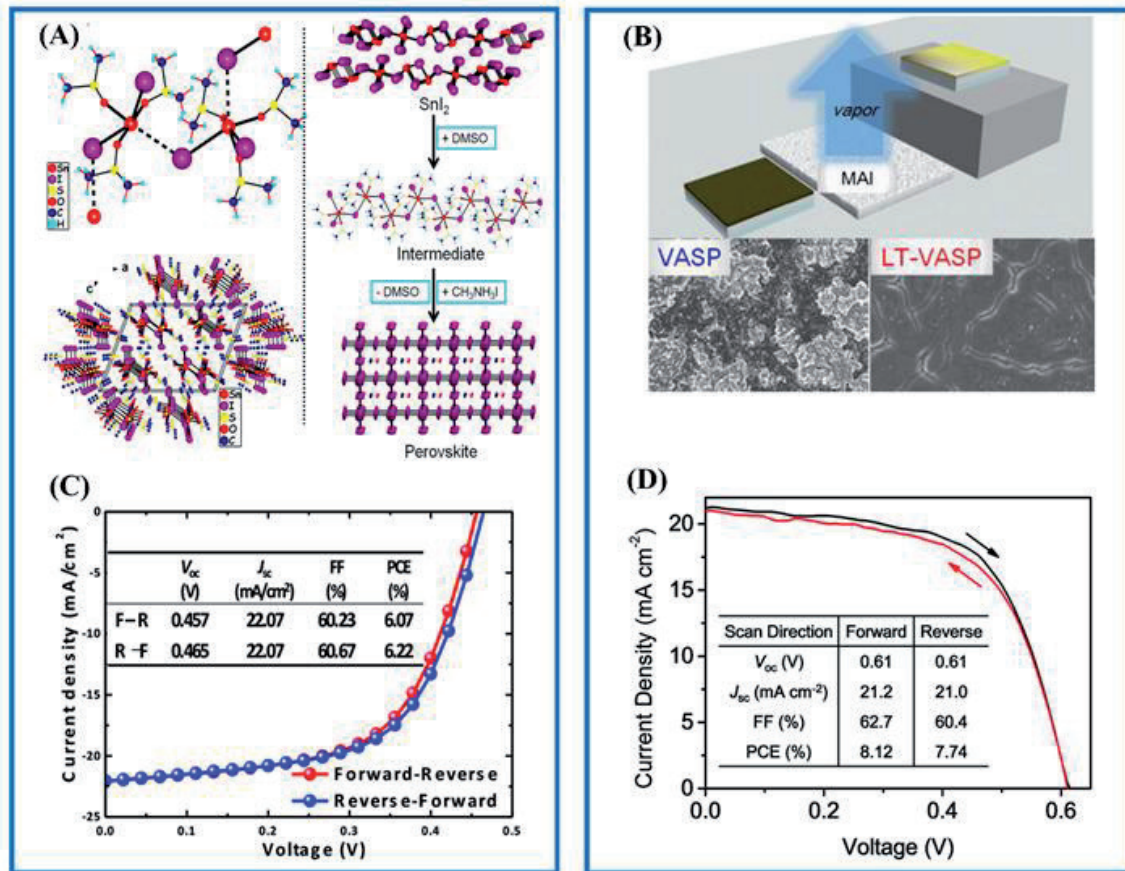


Figure 2. (A) Transient terahertz photoconductivity and simulated crystal structure of MASnI_3 . (B) Time-resolved photoluminescence for 20 mol (%) SnF_2 -doped MASnI_3 thin film and schematic device illustration. Reprinted with permission from [30, 31].


Figure 3.

(A) The schematic illustrations of the $\text{SnI}(\text{DMSO})^{3+}$ ions linked with lone Γ ions, unit cell of $\text{SnI}_2 \cdot 3\text{DMSO}$, and the film formation of the MASnI_3 perovskite starting from SnI_2 through $\text{SnI}_2 \cdot 3\text{DMSO}$ intermediate. (B) Scanning electron microscopy images of MASnI_3 thin films obtained through low-temperature vapor-assisted solution process and vapor-assisted solution method. (C) Current–voltage characteristic curves of the cell based on FASnI_3 with 10% SnF_2 additives. (D) Current–voltage curves of the best device based on $(\text{FA})_{0.75}(\text{MA})_{0.25}\text{SnI}_3$ perovskite. Reprinted with permission from [40–43].

inhibit the phase separation caused by excess SnF_2 (**Figure 4A**) [45]. Furthermore, the built-in potential can also be optimized through SnF_2 and thus high open-circuit voltage of the device by energetic landscape alignments [46] as illustrated in (**Figure 4B**). Besides SnF_2 , other additives such as SnBr_2 , SnI_2 , and SnCl_2 have also been explored where SnCl_2 exhibits the highest stability by inhibiting the decomposition/oxidation [34, 47]. Moreover, the employment of hypophosphorous acid in $\text{CsSnI}_2\text{Br}_2$ showed seed-like perovskite where Sn^{2+} oxidation was significantly reduced [48]. As a result, the charge recombination rate was decreased by fourfold compared to the control devices. The as-prepared cells displayed excellent oxygen-moisture stability at ambient conditions and thermal stability in vacuum environment.

The inclusion of large ammonium cations for tuning the dimensionality or generating massive Schottky defects has also been tested in Sn-based perovskites to optimize the device performance. For example, a different ratio of phenylethylammonium (PEA) as a cation can yield perovskites with two-dimensional, three-dimensional, and three-dimensional-two-dimensional-mixed dimensionalities. The high-quality thin film of the mixed PEA-FA perovskite (20% of PEA) delivered a stable device efficiency of 5.9% [49]. The composition of ethylenediammonium (en) and formamidinium (FA) in $\text{FASnI}_3/\text{MASnI}_3/\text{CsSnI}_3$ crystal indicates no effect on the dimensionality of the perovskite because the size of en is too large for the unit cell cage and it can remove a certain $\{\text{SnI}\}^+$ species. Here, the point defects are recognized as the Schottky defects. However, the optimized devices based on $\{\text{en}\}$ MASnI_3 and $\{\text{en}\}$ FASnI_3 showed efficiency of 6.6 and 7.1%, respectively [50, 51].

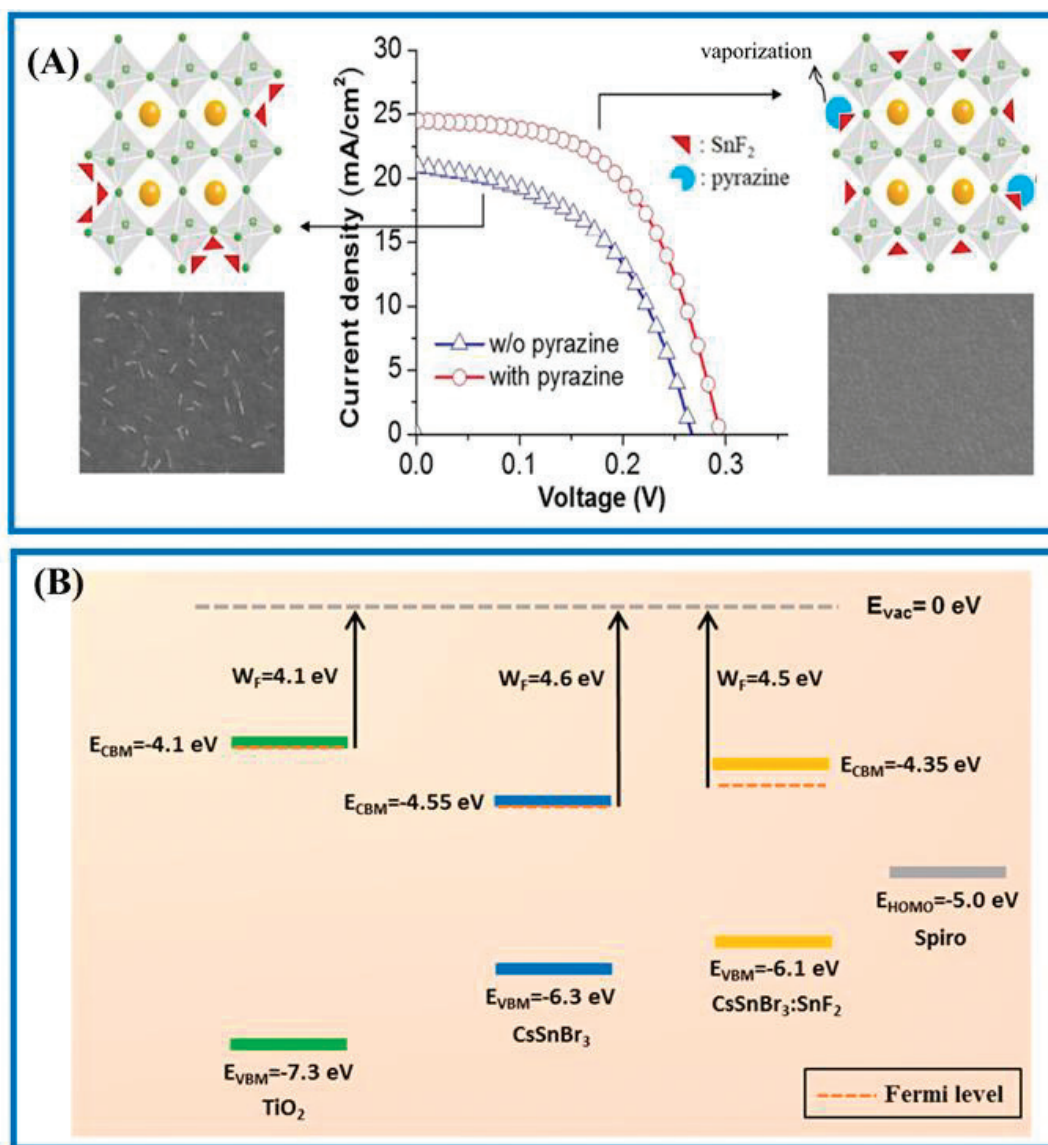


Figure 4. (A) Schematic crystal structure of FASnI₃ with SnF₂ and SnF₂-pyrazine complex with corresponding scanning electron microscopy images. (B) Representation of energetic landscapes of the TiO₂, pure CsSnBr₃, and 20 mol (%) of SnF₂ in CsSnBr₃ and spiro-OMeTAD with respect to vacuum level. Reprinted with permission from [45, 46].

3. Ge-, Bi-, Sb-, and Cu-based perovskites

Although Sn-based PSC has achieved PCE over 8%, the oxidation of Sn and degradation of the perovskite still need to be addressed. In this context, other metal halide perovskites such as Ge, Bi, Sb, and Cu are considered as potential candidates to replace Pb element in the perovskite crystal. As Ge 4 s has higher orbital energy compared to Pb 6 s and Sn 5 s, thus Ge-based perovskites should exhibit smaller bandgaps. However, in practice the Ge-based perovskites such as CsGeI₃, MAgGeI₃, and FAGeI₃ displayed larger bandgaps (i.e., 1.63, 2.0, and 2.35 eV) than that of CH₃NH₃SnI₃ (1.30 eV) and CH₃NH₃PbI₃ (1.55 eV) [52]. The difference between experimental data and what we expected from high orbital energy is mainly due to the structural distortion of [GeI₆] octahedral as the small ionic radius (0.73 Å) of Ge²⁺ substituting the bigger ionic radius of Pb²⁺ (1.19 Å) or Sn²⁺ (1.02 Å) [53]. Additionally, the Ge-based perovskites crystallize in polar space groups [54]. The Ge²⁺ cation cannot sustain at the center of octahedron and forms three long Ge—I bonds (2.73–2.77 Å) and three short Ge—I bonds (3.26–3.58 Å) [53]. This means that the Ge cation cannot maintain

the desirable octahedral crystal structure which may be one of the reasons for poorer device performance (the best PCE up to 0.2% so far) as compared to Pb- or Sn-based perovskite [52].

Furthermore, Bi and Sb can form $A_3B_2X_9$ perovskite structure such as $A_3Bi_2X_9$ and $A_3Sb_2X_9$ [55, 56]. These perovskites typically form low-dimensional perovskites with two polymorphs. Devices fabricated with $Cs_3Bi_2I_9$, $(MA)_3Bi_2I_9$, and $MA_3Bi_2I_{9-x}Cl_x$ (hexagonal phase and $P63/mm(194)$ space group) delivered PCE of 1, 0.33, and 0.38%, respectively [35]. The highest performance in the case of $Cs_3Bi_2I_9$ perovskite was attributed to the low non-radiative recombination. The A cation has also a crucial role in the formation of $Cs_3Sb_2I_9$ perovskite. For instance, the mixture of Cs^+ and MA^+ cations forms dimer phases [57], which is structurally different phase from rubidium (Rb) as the A cation. The DFT analysis about the dimer and layer forms of $A_3Sb_2I_9$ ($A = Cs$ or Rb) indicated much preference of Rb-based systems (with formation energy of 0.25 eV) as layered phase compared to Cs-based perovskite (formation energy of 0.1 eV). Thus the $Rb_3Sb_2I_9$ perovskite in PSC showed a PCE of 0.66% [57]. Recently, our research group fabricated Cu-based hybrid materials denoted as $(MA)_2CuX$ (where $X = Cl_4, I_2Cl_2,$ or Br_2Cl_2) to replace Pb [15]. It was revealed that chlorine (Cl^-) in the perovskite crystal has a critical role in the stabilization of the as-prepared materials. The corresponding PCEs of the devices are depicted in **Figure 5**.

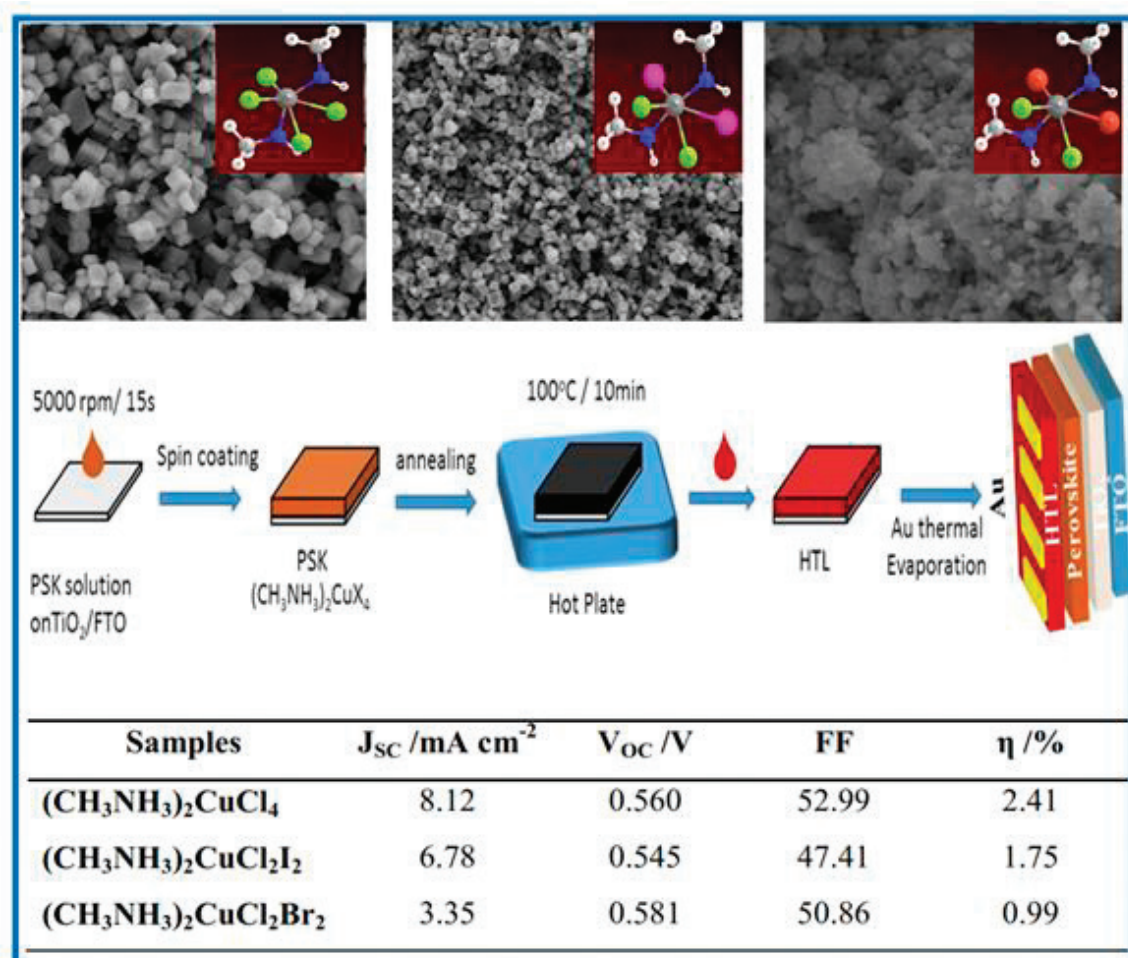


Figure 5. SEM micrographs of $(MA)_2CuCl_4$, $(MA)_2CuI_2Cl_2$, and $(MA)_2CuBr_2Cl_2$ with their chemical structures, respectively. Schematic illustration of the as-fabricated devices along with photovoltaic parameter table. Reprinted with permission from [35].

4. Summary and future outlook

It is concluded that the nontoxic elements should form octahedral crystal structure with halides. Besides the bandgaps, structural/electronic dimensionality, crystal defects, carrier motilities, and high-quality film formation of Pb-free perovskites are equally important. Although Sn is widely used to replace Pb in perovskites, it oxidizes from Sn^{2+} to Sn^{4+} and leads to high charge recombination and poor device performance. In addition, the fast crystallization of Sn-based perovskites forms pores in their thin films that deteriorate the solar cell performance. Thus, additives and additional solvent such as SnF_2 , SnCl_2 , SnF_2 -pyrazine complex, $\text{SnI}_2(\text{DMSO})_x$ complex, and HPA can be optimized to inhibit the oxidation reaction and control film growth rate. Another severe effect found in the Sn-based device is the hysteresis that is mostly associated with the imbalance charge transport and defects. In this context, mitigation of ion migration within perovskite and interfacial engineering by using suitable charge-transporting materials can reduce the hysteresis effect.

The Ge-based perovskites exhibit larger bandgaps which can deliver high open-circuit voltage compared to Sn-based perovskite. However, they also show severe oxidation. Alternatively, perovskite structure with trivalent $\text{Bi}^{3+}/\text{Sb}^{3+}$ cations can be designed. Copper is also a promising alternative to Pb in mixed halide perovskites where the Cu reduction can be decreased and the material stability as well as the perovskite crystallization can be enhanced by manipulating the halide ions. Replacing the toxic Pb in perovskite crystals with environmentally friendly, nontoxic, earth-abundant, and cost-effective materials such as transition metals (Fe^{2+} , Zn^{2+} , Cu^{2+} , etc.) is an important target for sustainable energy perspectives.

Acknowledgements

This work is supported partially by the National Natural Science Foundation of China (Grant nos. 51772096), Natural Science Foundation of Beijing Municipality (L172036), Joint Funds of the Equipment Pre-Research and Ministry of Education (6141A020225), Par-Eu Scholars Program, Science and Technology Beijing 100 Leading Talent Training Project, Beijing Municipal Science and Technology Project (Z161100002616039), Fundamental Research Funds for the Central Universities (2016JQ01, 2017ZZD02), and NCEPU “Double First-Class” Graduate Talent Cultivation Program.

Conflict of interest

The authors declare no conflict of interest.


IntechOpen

Author details

Sajid Sajid, Jun Ji, Haoran Jiang, Xin Liu, Mingjun Duan, Dong Wei, Peng Cui, Hao Huang, Shangyi Dou, Lihua Chu, Yingfeng Li, Bing Jiang and Meicheng Li*
State Key Laboratory of Alternate Electrical Power System with Renewable Energy Sources, School of Renewable Energy, North China Electric Power University, Beijing, China

*Address all correspondence to: mcli@ncepu.edu.cn

IntechOpen

© 2018 The Author(s). Licensee IntechOpen. This chapter is distributed under the terms of the Creative Commons Attribution License (<http://creativecommons.org/licenses/by/3.0>), which permits unrestricted use, distribution, and reproduction in any medium, provided the original work is properly cited. 

References

- [1] Kojima A, Teshima K, Shirai Y, Miyasaka T. Organometal halide perovskites as visible-light sensitizers for photovoltaic cells. *Journal of the American Chemical Society*. 2009;**131**(17):6050-6051
- [2] Cui P, Wei D, Ji J, et al. Highly efficient electron-selective layer free perovskite solar cells by constructing effective p-n heterojunction. *Solar RRL*. 2017;**1**(2):1600027
- [3] Wei D, Ji J, Song D, et al. A TiO₂ embedded structure for perovskite solar cells with anomalous grain growth and effective electron extraction. *Journal of Materials Chemistry A*. 2017;**5**(4):1406-1414
- [4] Wei D, Ma F, Wang R, et al. Ion-migration inhibition by the cation- π interaction in perovskite materials for efficient and stable perovskite solar cells. *Advanced Materials*. 2018;**30**(31):1707583
- [5] Sajid S, Elseman AM, Huang H, et al. Breakthroughs in NiO_x-HTMs towards stable, low-cost and efficient perovskite solar cells. *Nano Energy*. 2018;**51**:408-424
- [6] Elseman AM, Sharmoukh W, Sajid S, et al. Superior stability and efficiency over 20% perovskite solar cells achieved by a novel molecularly engineered Rutin-AgNPs/thiophene copolymer. *Advanced Science*. 2018;**5**(11):1800568
- [7] Available from: <https://www.nrel.gov/pv/assets/pdfs/pv-efficiencies-07-17-2018.pdf>
- [8] Song D, Cui P, Wang T, et al. Managing carrier lifetime and doping property of lead halide perovskite by postannealing processes for highly efficient perovskite solar cells. *The Journal of Physical Chemistry C*. 2015;**119**(40):22812-22819
- [9] Elseman A, Ji J, Dou S, et al. Novel hole transport layer of nickel oxide composite with carbon for high-performance perovskite solar cells. *Chinese Physics B*. 2018;**27**(1):017305
- [10] Sajid S, Elseman AM, Ji J, et al. Computational study of ternary devices: Stable, low-cost, and efficient planar perovskite solar cells. *Nano-Micro Letters*. 2018;**10**(3):51
- [11] Elseman AM, Sajid DW, Shalan AE, Rashad MM, Li M. Pathways towards high-stable, low-cost and efficient perovskite solar cells. In: *Emerging Solar Energy Materials*. IntechOpen; 2018
- [12] Yue S, Liu K, Xu R, et al. Efficacious engineering on charge extraction for realizing highly efficient perovskite solar cells. *Energy & Environmental Science*. 2017;**10**(12):2570-2578
- [13] Zhang Z, Yue X, Wei D, et al. DMSO-based PbI₂ precursor with PbCl₂ additive for highly efficient perovskite solar cells fabricated at low temperature. *RSC Advances*. 2015;**5**(127):104606-104611
- [14] Elseman AM, Rashad MM, Hassan AM. Easily attainable, efficient solar cell with mass yield of nanorod single-crystalline organo-metal halide perovskite based on a ball milling technique. *ACS Sustainable Chemistry & Engineering*. 2016;**4**(9):4875-4886
- [15] Elseman AM, Shalan AE, Sajid S, Rashad MM, Hassan AM, Li M. Copper-substituted lead perovskite materials constructed with different halides for working (CH₃NH₃)₂CuX₄-based perovskite solar cells from experimental and theoretical view. *ACS Applied Materials & Interfaces*. 2018;**10**(14):11699-11707
- [16] Babayigit A, Ethirajan A, Muller M, Conings B. Toxicity of organometal

- halide perovskite solar cells. *Nature Materials*. 2016;**15**:247
- [17] Kadro JM, Pellet N, Giordano F, et al. Proof-of-concept for facile perovskite solar cell recycling. *Energy & Environmental Science*. 2016;**9**(10):3172-3179
- [18] Sajid EAM, Ji J, et al. Novel hole transport layer of nickel oxide composite with carbon for high-performance perovskite solar cells. *Chinese Physics B*. 2018;**27**(1):17305-017305
- [19] Sajid S, Elseman AM, Wei D, et al. NiO@Carbon spheres: A promising composite electrode for scalable fabrication of planar perovskite solar cells at low cost. *Nano Energy*. 2018/11/03/
- [20] Gao P, Grätzel M, Nazeeruddin MK. Organohalide lead perovskites for photovoltaic applications. *Energy & Environmental Science*. 2014;**7**(8):2448-2463
- [21] Zhao Y, Zhu K. Organic-inorganic hybrid lead halide perovskites for optoelectronic and electronic applications. *Chemical Society Reviews*. 2016;**45**(3):655-689
- [22] Tsai H, Nie W, Blancon J-C, et al. High-efficiency two-dimensional Ruddlesden-Popper perovskite solar cells. *Nature*. 2016;**536**:312
- [23] Xiao Z, Meng W, Wang J, Mitzi DB, Yan Y. Searching for promising new perovskite-based photovoltaic absorbers: The importance of electronic dimensionality. *Materials Horizons*. 2017;**4**(2):206-216
- [24] Yin W-J, Shi T, Yan Y. Unique properties of halide perovskites as possible origins of the superior solar cell performance. *Advanced Materials*. 2014;**26**(27):4653-4658
- [25] Ganose AM, Savory CN, Scanlon DO. Beyond methylammonium lead iodide: Prospects for the emergent field of ns(2) containing solar absorbers. *Chemical Communications*. 2016;**53**(1):20-44
- [26] Konstantakou M, Stergiopoulos T. A critical review on tin halide perovskite solar cells. *Journal of Materials Chemistry A*. 2017;**5**(23):11518-11549
- [27] Zuo F, Williams ST, Liang P-W, Chueh C-C, Liao C-Y, Jen AK-Y. Binary-metal perovskites toward high-performance planar-heterojunction hybrid solar cells. *Advanced Materials*. 2014;**26**(37):6454-6460
- [28] Bernal C, Yang K. First-principles hybrid functional study of the organic-inorganic perovskites $\text{CH}_3\text{NH}_3\text{SnBr}_3$ and $\text{CH}_3\text{NH}_3\text{SnI}_3$. *The Journal of Physical Chemistry C*. 2014;**118**(42):24383-24388
- [29] Umari P, Mosconi E, De Angelis F. Relativistic GW calculations on $\text{CH}_3\text{NH}_3\text{PbI}_3$ and $\text{CH}_3\text{NH}_3\text{SnI}_3$ perovskites for solar cell applications. *Scientific Reports*. 2014;**4**:4467
- [30] Noel NK, Stranks SD, Abate A, et al. Lead-free organic-inorganic tin halide perovskites for photovoltaic applications. *Energy & Environmental Science*. 2014;**7**(9):3061-3068
- [31] Ma L, Hao F, Stoumpos CC, Phelan BT, Wasielewski MR, Kanatzidis MG. Carrier diffusion lengths of over 500 nm in lead-free perovskite $\text{CH}_3\text{NH}_3\text{SnI}_3$ films. *Journal of the American Chemical Society*. 2016;**138**(44):14750-14755
- [32] Chiarella F, Zappettini A, Licci F, et al. Combined experimental and theoretical investigation of optical, structural, and electronic properties of $\text{CH}_3\text{NH}_3\text{SnX}_3$ thin films (X = Cl, Br). *Physical Review B*. 2008;**77**(4):045129
- [33] Fujihara T, Terakawa S, Matsushima T, Qin C, Yahiro M,

Adachi C. Fabrication of high coverage MASnI_3 perovskite films for stable, planar heterojunction solar cells. *Journal of Materials Chemistry C*. 2017;5(5):1121-1127

[34] Tsai C-M, Mohanta N, Wang C-Y, et al. Formation of stable tin perovskites co-crystallized with three halides for carbon-based mesoscopic lead-free perovskite solar cells. *Angewandte Chemie*. 2017;129(44):14007-14011

[35] Park B-W, Philippe B, Zhang X, Rensmo H, Boschloo G, Johansson EMJ. Bismuth based hybrid perovskites $\text{A}_3\text{Bi}_2\text{I}_9$ (A: methylammonium or cesium) for solar cell application. *Advanced Materials*. 2015;27(43):6806-6813

[36] Chen Z, Yu C, Shum K, et al. Photoluminescence study of polycrystalline CsSnI_3 thin films: Determination of exciton binding energy. *Journal of Luminescence*. 2012;132(2):345-349

[37] Shum K, Chen Z, Qureshi J, et al. Synthesis and characterization of CsSnI_3 thin films. *Applied Physics Letters*. 2010;96(22):221903

[38] Chung I, Song J-H, Im J, et al. CsSnI_3 : Semiconductor or metal? High electrical conductivity and strong near-infrared photoluminescence from a single material. High hole mobility and phase-transitions. *Journal of the American Chemical Society*. 2012;134(20):8579-8587

[39] Liu C, Li W, Fan J, Mai Y. A brief review on the lead element substitution in perovskite solar cells. *Journal of Energy Chemistry*. 2018;27(4):1054-1066

[40] Hao F, Stoumpos CC, Guo P, et al. Solvent-mediated crystallization of $\text{CH}_3\text{NH}_3\text{SnI}_3$ films for heterojunction depleted perovskite solar cells. *Journal of the American Chemical Society*. 2015;137(35):11445-11452

[41] Yokoyama T, Cao DH, Stoumpos CC, et al. Overcoming short-circuit in lead-free $\text{CH}_3\text{NH}_3\text{SnI}_3$ perovskite solar cells via kinetically controlled gas-solid reaction film fabrication process. *The Journal of Physical Chemistry Letters*. 2016;7(5):776-782

[42] Liao W, Zhao D, Yu Y, et al. Lead-free inverted planar formamidinium tin triiodide perovskite solar cells achieving power conversion efficiencies up to 6.22%. *Advanced Materials*. 2016;28(42):9333-9340

[43] Zhao Z, Gu F, Li Y, et al. Mixed-organic-cation tin iodide for lead-free perovskite solar cells with an efficiency of 8.12%. *Advanced Science*. 2017;4(11):1700204

[44] Yokoyama T, Song T-B, Cao DH, Stoumpos CC, Aramaki S, Kanatzidis MG. The origin of lower hole carrier concentration in methylammonium tin halide films grown by a vapor-assisted solution process. *ACS Energy Letters*. 2017;2(1):22-28

[45] Lee SJ, Shin SS, Kim YC, et al. Fabrication of efficient formamidinium tin iodide perovskite solar cells through SnF_2 -pyrazine complex. *Journal of the American Chemical Society*. 2016;138(12):3974-3977

[46] Gupta S, Bendikov T, Hodes G, Cahen D. CsSnBr_3 , a lead-free halide perovskite for long-term solar cell application: Insights on SnF_2 addition. *ACS Energy Letters*. 2016;1(5):1028-1033

[47] Marshall KP, Walker M, Walton RI, Hatton RA. Enhanced stability and efficiency in hole-transport-layer-free CsSnI_3 perovskite photovoltaics. *Nature Energy*. 2016;1:16178

[48] Li W, Li J, Li J, Fan J, Mai Y, Wang L. Additive-assisted construction of all-inorganic $\text{CsSnI}_3\text{Br}_2$ mesoscopic perovskite solar cells with superior

thermal stability up to 473 K. *Journal of Materials Chemistry A*. 2016;**4**(43):17104-17110

[49] Liao Y, Liu H, Zhou W, et al. Highly oriented low-dimensional tin halide perovskites with enhanced stability and photovoltaic performance. *Journal of the American Chemical Society*. 2017;**139**(19):6693-6699

[50] Ke W, Stoumpos CC, Zhu M, et al. Enhanced photovoltaic performance and stability with a new type of hollow 3D perovskite FASnI_3 . *Science Advances*. 2017;**3**(8):1701293

[51] Ke W, Stoumpos CC, Spanopoulos I, et al. Efficient lead-free solar cells based on hollow MASnI_3 perovskites. *Journal of the American Chemical Society*. 2017;**139**(41):14800-14806

[52] Krishnamoorthy T, Ding H, Yan C, et al. Lead-free germanium iodide perovskite materials for photovoltaic applications. *Journal of Materials Chemistry A*. 2015;**3**(47):23829-23832

[53] Lu X, Zhao Z, Li K, et al. First-principles insight into the photoelectronic properties of Ge-based perovskites. *RSC Advances*. 2016;**6**(90):86976-86981

[54] Lin Z-G, Tang L-C, Chou C-P. Characterization and properties of novel infrared nonlinear optical crystal $\text{CsGe}(\text{Br}_x\text{Cl}_{1-x})_3$. *Inorganic Chemistry*. 2008;**47**(7):2362-2367

[55] Zhang X, Wu G, Gu Z, et al. Active-layer evolution and efficiency improvement of $(\text{CH}_3\text{NH}_3)_3\text{Bi}_2\text{I}_9$ -based solar cell on TiO_2 -deposited ITO substrate. *Nano Research*. 2016;**9**(10):2921-2930

[56] Saparov B, Hong F, Sun J-P, et al. Thin-film preparation and characterization of $\text{Cs}_3\text{Sb}_2\text{I}_9$: A lead-free layered perovskite

semiconductor. *Chemistry of Materials*. 2015;**27**(16):5622-5632

[57] Harikesh PC, Mulmudi HK, Ghosh B, et al. Rb as an alternative cation for templating inorganic lead-free perovskites for solution processed photovoltaics. *Chemistry of Materials*. 2016;**28**(20):7496-7504